JOC Article

Theoretical Study of the Effect of Coordinating Solvent on Ion Pair S_N2 Reactions: The Role of Unsymmetrical Transition Structures

Andrew Streitwieser* and Elambalassery G. Jayasree

Department of Chemistry, University of California, Berkeley, California 94720-1460

astreit@berkeley.edu

Received December 14, 2006

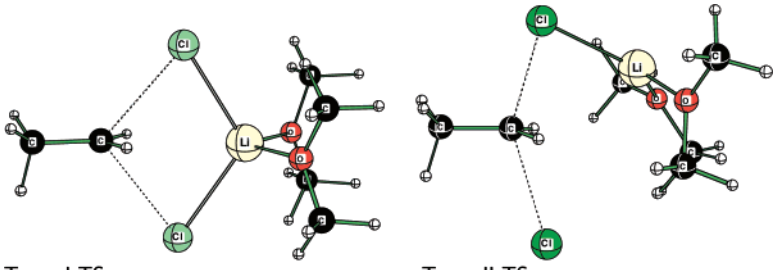

Computations are reported at the HF/6-31+g* level for ion pair S_N2 reactions of methyl, ethyl, *n*-propyl, isopropyl, and allyl halides with LiX·E, LiX·2E, and LiX·3E (X = F, Cl, Br; E = dimethyl ether as a model for THF). Some calculations were also done at the MP2, B3LYP, and mPW1PW91 levels. In addition to normal S_N2-type (type I) transition structures (TSs), novel unsymmetrical TSs were found in which the Li is coordinated to a single halide. With LiX·2E, such structures are already competitive with the type I structures, and with LiX·3E, only the type II structures were found. With incorporation of dielectric solvation, the type II structures are relatively even more stable. The results suggest that such structures are better models for ion pair displacement reactions in ethereal solvents.

Introduction

The importance of solvation effects on S_N2 reactions of ions has given rise to many theoretical studies.[1−4] In solvents of lower polarity, ion pairs are known to be important,[5,6]—but theoretical studies of ion pair reactions are scarce.[7−13] Ion pairs are neutral substrates and are expected to be less sensitive to solvent; however, they are dipoles and solvation is doubtless not negligible. Nevertheless, only recently has the effect of solvent on ion pair S_N2 reactions been explored computationally and then only with a polarized continuum model.[14] Computational studies on ion pair reactions of alkyl halides and metal halides in the gaseous unsolvated state show highly bent transition states with high-energy barriers. In this paper, we present a study of the effect of solvation on the transition structures, energetics, and reaction mechanisms of ion pair S_N2 displacement reactions between alkyl halides, RX, and lithium halides, LiX (X = F, Cl, Br) in a dipolar aprotic solvent, dimethyl ether (Me_2O). We chose an ether solvent although many experimental studies of ion pair S_N2 reactions involve alcohols. Those studies generally involved both ion pairs and free ions; accordingly, the ion pairs involved might be "loose"

(1) Laerdahl, J. K.; Uggerud, E. *Int. J. Mass Spectrom.* **2002**, *214*, 277−314.
(2) Dedieu, A.; Veillard, A. In *Quantum Theory of Chemical Reactions*; Reidel: Dordrecht, 1979; Vol. 1, p 69.
(3) Minkin, V. I.; Simkin, B. Y.; Minyaev, R. M. In *Quantum Chemistry of Organic Compounds*; Springer-Verlag: New York, 1990; p 116.
(4) Shaik, S. S.; Schlegel, H. B.; Wolfe, S. *Theoretical Aspects of Physical Organic Chemistry. The SN2 mechanism*; Wiley: New York, 1992.
(5) Acree, S. F. *Am. Chem. J.* **1912**, *48*, 352−380.
(6) Winstein, S.; Savedoff, L. G.; Smith, S. G.; Stevens, I. D. R.; Gall, J. S. *Tetrahedron Lett.* **1960**, *9*, 24−30.
(7) Streitwieser, A.; Choy, G. S.-C.; Abu-Hasanayn, F. *J. Am. Chem. Soc.* **1997**, *119*, 5013−5019.
(8) Harder, S.; Streitwieser, A.; Petty, J. T.; Schleyer, P. V. *J. Am. Chem. Soc.* **1995**, *117*, 3253−3259.
(9) Leung, S. S.-W.; Streitwieser, A. *J. Comput. Chem.* **1998**, *19*, 1325−1336.
(10) Ren, Y.; Chu, S.-Y. *Chem. Phys. Lett.* **2003**, *376*, 524−531.
(11) Ren, Y.; Chu, S.-Y. *J. Comput. Chem.* **2004**, *25*, 461−471.
(12) Zhu, H.-j.; Ren, Y.; Ren, J. *J. Mol. Struct.: THEOCHEM* **2004**, *686*, 65−70.
(13) Zhu, H.-j.; Ren, Y.; Ren, J.; Chu, S.-Y. *Int. J. Quantum Chem.* **2005**, *101*, 104−112.
(14) Ren, Y.; Li, M.; Wong, N.-B.; Chu, S.-Y. *J. Mol. Model.* **2006**, *12*, 182−189.

10.1021/jo0625709 CCC: $37.00
Published on Web 02/01/2007

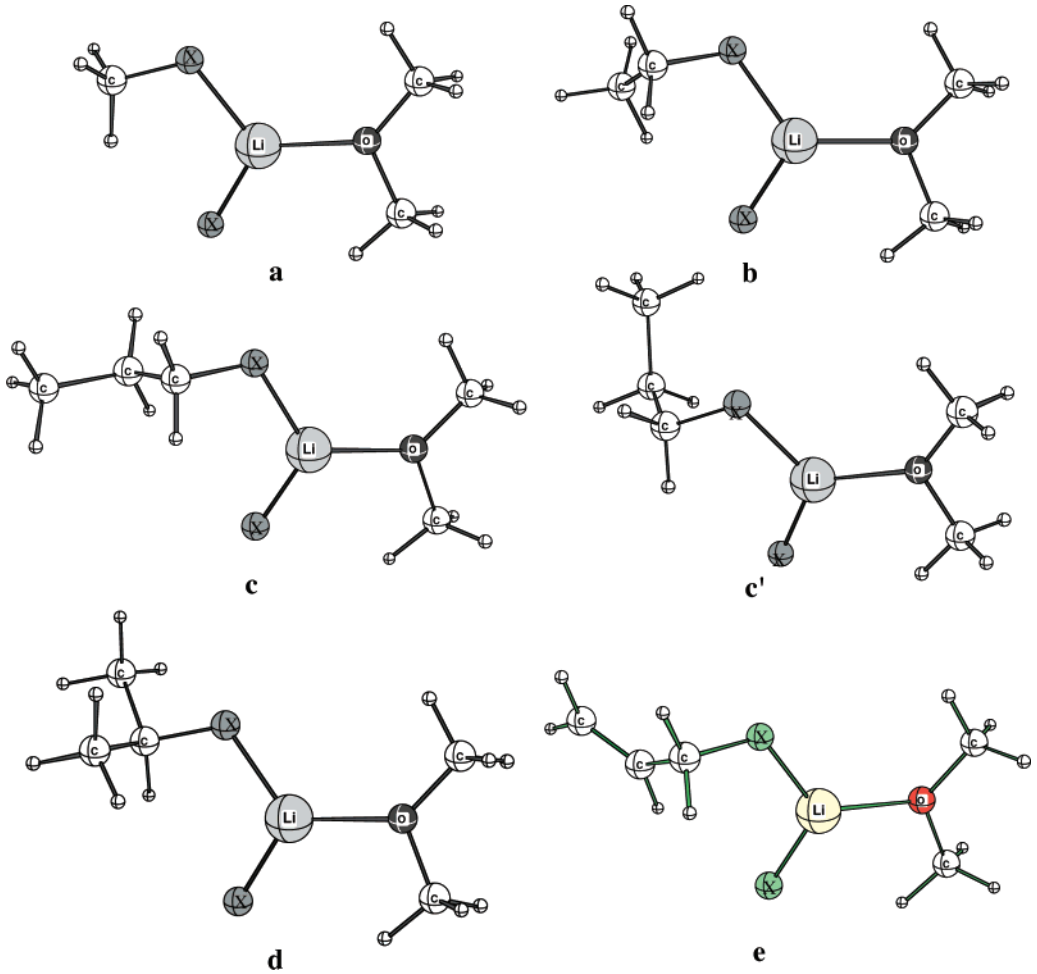

FIGURE 1. Optimized reaction complexes with monosolvation for RX−LiX·E reaction systems (X = F, Cl, Br). Letters refer to complexes with LiX·E and alkyl halides: a, methyl; b, ethyl; c and c′, *n*-propyl; d, isopropyl; e, allyl.

or solvent-separated. Moreover, most alkylation reactions of alkali enolates, that clearly involve contact ion pairs, make use of ether solvents, particularly THF. Dimethyl ether is an effective and common computational model for THF.[15] Our computational studies of ion pair S_N2 reactions of alkali enolates are still ongoing and will be presented later. In the present study, we consider narcissistic and some nonnarcissistic reactions of some alkyl halides with lithium halides.

One aspect of solvation was treated by specific coordination of metal with the solvent dimethyl ether, E. Related microsolvated gas-phase studies of ionic S_N2 reactions are known in the literature, both experimentally and theoretically, and have provided enhanced understanding of the microscopic dependence of reactivity toward solvation in going from the gas phase.[16] To include the effects of bulk solvation, the reactions were also computed with polarized continuum models (PCMs) that depend on the dielectric constant of the solvent.[17] Because the ion pair reactions involve neutral species that are dipolar or quadrupolar throughout the reaction, the dielectric effect is less important here than for ionic reactions. We had learned this in a previous study of coordination and dielectric solvation of lithium ion pairs of enolate aggregates and complexes.[18] This two-pronged approach was applied in the present study. The transition structures were characterized for each microsolvated reaction considered, and the reaction path was followed for several cases by intrinsic reaction coordinate (IRC) calculations.

Computational Methodology

Optimization of structures involved was done at the RHF/6-31+g*[19,20] level using various versions of Gaussian up to Gaussian 03.[21] For the prototypical reaction of methyl chloride with solvated lithium chloride, MeCl + LiCl·*n*E, additional calculations were added for comparison at the hybrid density functional methods, B3LYP and mPW1PW91. B3LYP is a common hybrid method, and mPW1PW91 has been specially calibrated for S_N2 reactions.[22] Transition structures (TSs) and minima were characterized by vibrational frequency analysis. IRC calculations were carried out in the forward and reverse directions at the same level of theory

(15) Streitwieser, A. *J. Mol. Model.* **2006**, *12*, 673−680.
(16) Bogdanov, B.; McMahon, T. B. *Int. J. Mass Spectrom.* **2005**, *241*, 205−223.
(17) Tomasi, J.; Mennucci, B.; Cammi, R. *Chem. Rev.* **2005**, *105*, 2999−3094.
(18) Pratt, L. M.; Streitwieser, A. *J. Org. Chem.* **2003**, *68*, 2830−2838.
(19) Clark, T.; Chandrasekhar, J.; Spitznagel, G. W.; Schleyer, P. v. R. *J. Comput. Chem.* **1983**, *4*, 294−301.
(20) Frisch, M. J.; Pople, J. A.; Binkley, J. S. *J. Chem. Phys.* **1984**, *80*, 3265−3269.
(21) Frisch, M. J. et. al *Gaussian 03*, revision C.02; Gaussian, Inc.: Wallingford, CT, 2004.
(22) Kormos, B. L.; Cramer, C. J. *J. Org. Chem.* **2003**, *68*, 6375−6386.
(23) Gonzalez, C.; Schlegel, H. B. *J. Chem. Phys.* **1989**, *90*, 2154−2161.

TABLE 1. Various Energy Barriers Calculated in kcal/mol[a]

	$\Delta E^{\ddagger}$			ΔE^{*}					
reaction·*n*E	I	II	$\Delta E^{\ddagger gas}$	I	II	ΔE^{*gas}	ΔE^{rc}	$\Delta E^{rc,gas}$	ΔE^{ts}
$CH_3F-LiF\cdot E$	66.69	61.45	64.48	54.90	49.66	49.75	−11.79	−14.73	5.24
		(64.56)			(48.00)				
·2E	68.21	53.30		60.99	46.08		−7.22		14.91
					(45.81)				
·3E		44.62		64.27	42.90		−1.72		21.37
$CH_3Cl-LiCl\cdot E$	48.27	48.34	47.75	40.56	40.62	36.39	−7.71	−11.36	−0.06
	40.62	*39.54*		*31.90*	*30.82*				*1.08*
		(47.28)			(37.20)				
·2E		41.11		[b]	36.50		−4.61		
		33.06		[b]	*27.83*				
		(40.72)			(33.73)				
·3E		35.91		[b]	32.27		−3.65		
		29.02			*25.58*				
		(35.45)			(31.20)				
$CH_3Br-LiBr\cdot E$	43.39	44.48	43.06	31.26	32.35	27.24	−12.13	−15.82	−1.10
·2E		38.47		[b]	26.72		−11.74		
·3E		29.08		[b]	23.33		−5.76		
$C_2H_5F-LiF\cdot E$	55.95	59.78	53.03	43.51	47.33	37.32	−12.45	−15.71	−3.82
·2E	58.31	50.52		50.71	42.92		−7.60		7.80
·3E		43.79		[b]	41.73		−2.06		
$C_2H_5Cl-LiCl\cdot E$	35.97	43.90	34.46	27.47	35.40	22.03	−8.50	−12.43	−7.93
	32.47	(45.68)		*22.93*	[c]				
	(42.50)			(31.55)	(34.72)				
·2E	37.57	37.34		32.53	32.30		−5.04		0.23
		31.27		[b]	*25.65*				
		(39.56)			(32.00)				
·3E		33.62		[b]	29.80		−3.82		
		28.11			*24.60*				
		(34.86)			(30.56)				
$C_2H_5Br-LiBr\cdot E$	33.38		30.56	19.06	[c]	14.36	−14.32	−16.20	
·2E	35.09	35.93		21.08	21.92		−14.01		−0.84
·3E		30.51		[b]	20.56		−9.95		
n-C_3H_7F-$LiF\cdot E$	56.28		53.11	43.72	[c]	37.29	−12.55	−15.82	
I′·E	54.83		51.75	42.43		36.08	−12.41	−15.67	
n-$C_3H_7Cl-LiCl\cdot E$	36.67		34.87	27.97	[c]	22.18	−8.70	−12.69	
I′·E	34.59		33.01	26.00		20.37	−8.59	−12.64	
n-$C_3H_7Br-LiBrI'\cdot E$	32.27		31.31	18.02	[c]	13.20	−14.25	−18.11	
i-$C_3H_7F-LiF\cdot E$	47.26	61.78	43.65	34.44	48.97	27.27	−12.82	−16.38	−14.53
·2E	51.3	55.2		42.91	46.81		−8.39		1.53
·3E		47.97			43.61		−4.36		2.68
i-$C_3H_7Cl-LiCl\cdot E$	26.31		23.67	17.28	[c]	10.43	−9.03	−13.24	
	29.21	(47.53)		*18.95*	*28.72*				*−9.77*
	(37.20)			(25.78)	(36.11)				(−10.33)
·2E	29.42	35.59		24.14	30.31		−5.28		−6.17
	30.88	*33.36*		*24.83*	*27.31*				*−2.48*
	(40.12)	(41.21)		(32.32)	(33.41)				(−1.09)
·3E		31.61		[b]	27.67		−3.94		
		(35.71)			(31.21)				
i-$C_3H_7Br-LiBr\cdot E$	25.65		23.12	11.31	[c]	4.80	−14.34	−18.32	
·2E	27.64	32.65		14.85	19.87		−12.79		−5.01
·3E		29.41		[b]	19.95		−9.46		
$C_3H_5F-LiF\cdot E$	48.63	61.70	44.54	35.72	48.80	28.54	−12.90	−16.06	−13.07
·2E	52.03	53.91		43.96	45.84		−8.07		−1.87
·3E				[b]	44.19				
$C_3H_5Cl-LiCl\cdot E$	27.81		24.87	19.22	[c]	12.49	−8.59	−12.41	
·2E	30.91			25.70	[c]		−5.20		
·3E				[b]	29.56				
$C_3H_5Br-LiBr\cdot E$	26.31		24.07	12.10	[c]	6.15	−14.21	−17.92	
·2E	29.22			15.25	[c]		−13.97		
·3E				[b]	20.08				

[a] $\Delta E^{\ddagger}$ (with respect to the reaction complex, RX·LiX·*n*E), ΔE^{*} (with respect to the separated reactants, RX + LiX·*n*E), and complexation energy ΔE^{rc} (with respect to the reactants) for the reactions RX + LiX·*n*E (E = dimethyl ether) at RHF/6-31+G(d). The relative TS energies, ΔE^{ts} (E(I)−E(II)) are also computed wherever applicable. The corresponding energy barriers in the gas phase (without a coordinating solvent) are also given for comparison as $\Delta E^{rc,gas}$. Calculations are done using the total energy including the unscaled zero point energy at HF/6-31+G* (values in italics are B3LYP/6-31+G*, and those in parentheses are mPW1PW91/6-31G* values). [b] Converged to type II. [c] Converged to type I.

TABLE 2. Some Bond Lengths and Angles of Transition Structures and Reaction Complexes (rc) of MeCl + LiCl·*n*E (*n* = 1−3) Computed Using Various Methods[a]

reaction complexes	C−Cl$_1$	C−Cl$_2$	Li−Cl$_1$	Li−Cl$_2$	Li−O	Cl−C−Cl	Cl−Li−Cl
			MeCl + LiCl·Erc				
HF/6-31+G*	1.812	3.732	2.540	2.143	1.903	82.0	113.2
B3LYP/6-31+G*	1.832	3.613	2.477	2.127	1.896	84.0	114.5
mPW1PW91/6-31G*	1.785	3.539	2.466	2.124	1.886	84.7	112.1
HF/6-311+G**	1.816	3.729	2.500	2.126	1.911	81.2	114.2
			MeCl + LiCl·2Erc				
HF/6-31+G*	1.805	3.72	2.842	2.195	1.954, 1.978	84.7	103.7
B3LYP/6-31+G*	1.825	3.591	2.693	2.184	1.946, 1.979	85.4	105.5
mPW1PW91/6-31G*	1.779	3.516	2.606	2.174	1.927, 1.954	85.4	105.3
HF/6-311+G**	1.808	3.717	2.827	2.179	1.957, 1.983	84.2	104.0
			MeCl + LiCl·3Erc				
HF/6-31+G*	1.800	3.881	5.084	2.244	2.023, 2.011	110.4	70.2
B3LYP/6-31+G*	1.819	3.745	4.991	2.226	2.016, 2.008, 1.988	111.6	70.2
mPW1PW91/6-31G*	1.774	3.687	4.779	2.207	1.976, 1.981, 1.956	112.5	73.6
HF/6-311+G**	1.804	3.864	5.012	2.230	2.023, 2.011, 2.029	108.9	70.7
transition structures	**C−Cl$_1$**	**C−Cl$_2$**	**Li−Cl$_1$**	**Li−Cl$_2$**	**Li−O**	**Cl−C−Cl**	**Cl−Li−Cl**
			MeCl + LiCl·EI				
HF/6-31+G*	2.652		2.367		1.894	98.5	116.2
B3LYP/6-31+G*	2.488		2.438		1.872	117.6	121.6
mPW1PW91/6-31G*	not a TS						
MP2/6-31+G*	not a TS						
HF/6-311+G**	2.663		2.336		1.905	96.5	116.5
			MeCl + LiCl·EII				
HF/6-31+G*	2.149	2.632	2.229	4.584	1.841	163.3	79.8
B3LYP/6-31+G*	2.110	2.628	2.245	3.833	1.836	161.1	97.1
mPW1PW91/6-31G*	2.087	2.480	2.223	3.921	1.835	168.0	91.0
MP2/6-31+G*	2.128	2.478	2.182	3.942	1.787	169.7	92.5
HF/6-311+G**	2.147	2.623	2.201	4.672	1.854	164.6	77.9
			MeCl + LiCl·2EII				
HF/6-31+G*	2.211	2.559	2.308	4.449	1.913	164.8	82.3
B3LYP/6-31+G*	2.171	2.568	2.308	4.027	1.907, 1.904	163.6	91.4
mPW1PW91/6-31G*	2.140	2.44	2.281	4.063	1.901, 1.896	167.4	87.0
HF/6-311+G**	2.214	2.548	2.278	4.453	1.919, 1.916	165.3	82.3
			MeCl + LiCl·3EII				
HF/6-31+G*	2.195	2.574	2.397	5.213	1.999, 1.984	169.7	65.5
B3LYP/6-31+G*	2.105	2.637	2.406	4.982	1.982, 1.985, 1.962	168.6	69.6
mPW1PW91/6-31G*	2.103	2.482	2.353	4.857	1.956, 1.941	172.1	69.0
HF/6-311+G**	2.201	2.561	2.371	5.213	1.991, 2.000, 2.002	169.8	65.4

[a] All other parameters are given in the Supporting Information.

used for optimization.[23,24] Although the reaction complexes are less important in solution, microsolvated gas-phase reactions have been reported to show solvated S_N2 complexes as intermediates.[16] The energy barrier calculated as the difference between the reaction complex (RX·LiX·*n*E) and the TS is denoted as $\Delta E^{\ddagger}$, and the energy barrier calculated with respect to the reactants (RX + LiX·*n*E) is denoted as ΔE^{*}. Total energies including the unscaled zero-point energies were used to calculate the energy barriers. Dielectric solvation, the dielectric effects from the surrounding environment, was obtained using the CPCM polarizable conductor model[25] implemented in Gaussian 03 with the Cosmo keyword, in which the solvent cavity is formed as a surface of constant charge density around the solvated molecule. Free energies of solvation were calculated using single-point energies on the RHF/6-31+G* optimized geometry. The radii of the solvent molecules were taken from the parameters for THF. The united atom topological model[26] was used to build the cavity around each heavy atom. Because our systems are dipoles in relatively nonpolar solvents, the magnitudes of the dielectric solvation are relatively small and almost any PCM should give comparable results.

Calculations were done on methyl, ethyl, *n*-propyl, *i*-propyl, and allyl systems.

Results and Discussion

We consider first the narcissistic reactions of lithium halides with methyl halides.

In ethereal solutions, the lithium cation is usually considered to be tetracoordinated although the situation is less clear for lithium ion pair salts.[18] Our previous calculations of the effects of successive ether coordination with LiCl and LiBr suggest that there are significant populations of both LiX·2E and LiX·3E at normal temperatures. Thus, we studied the S_N2 reactions with both LiX·2E and LiX·3E as realistic models of the actual reactants. However, we include computations of LiX·E even though the lithium is only dicoordinated to demonstrate a progressive change from unsolvated to fully coordinated.

Reaction Complexes. In the gas phase, S_N2 reactions generally involve a complex between the reactants that can be considered as an encounter complex or "reaction complex",[27] a

(24) Gonzalez, C.; Schlegel, H. B. *J. Phys. Chem.* **1990**, *94*, 5523−5527.
(25) Barone, V.; Cossi, M. *J. Phys. Chem. A* **1998**, *102*, 1995−2001.
(26) Barone, V. M.; Cossi, M.; Tomasi, J. *J. Chem. Phys.* **1997**, *107*, 3210−3221.
(27) Olmstead, W. N.; Brauman, J. I. *J. Am. Chem. Soc.* **1977**, *99*, 4219−4228.
(28) Dedieu, A.; Veillard, A. *J. Am. Chem. Soc.* **1972**, *94*, 6730.

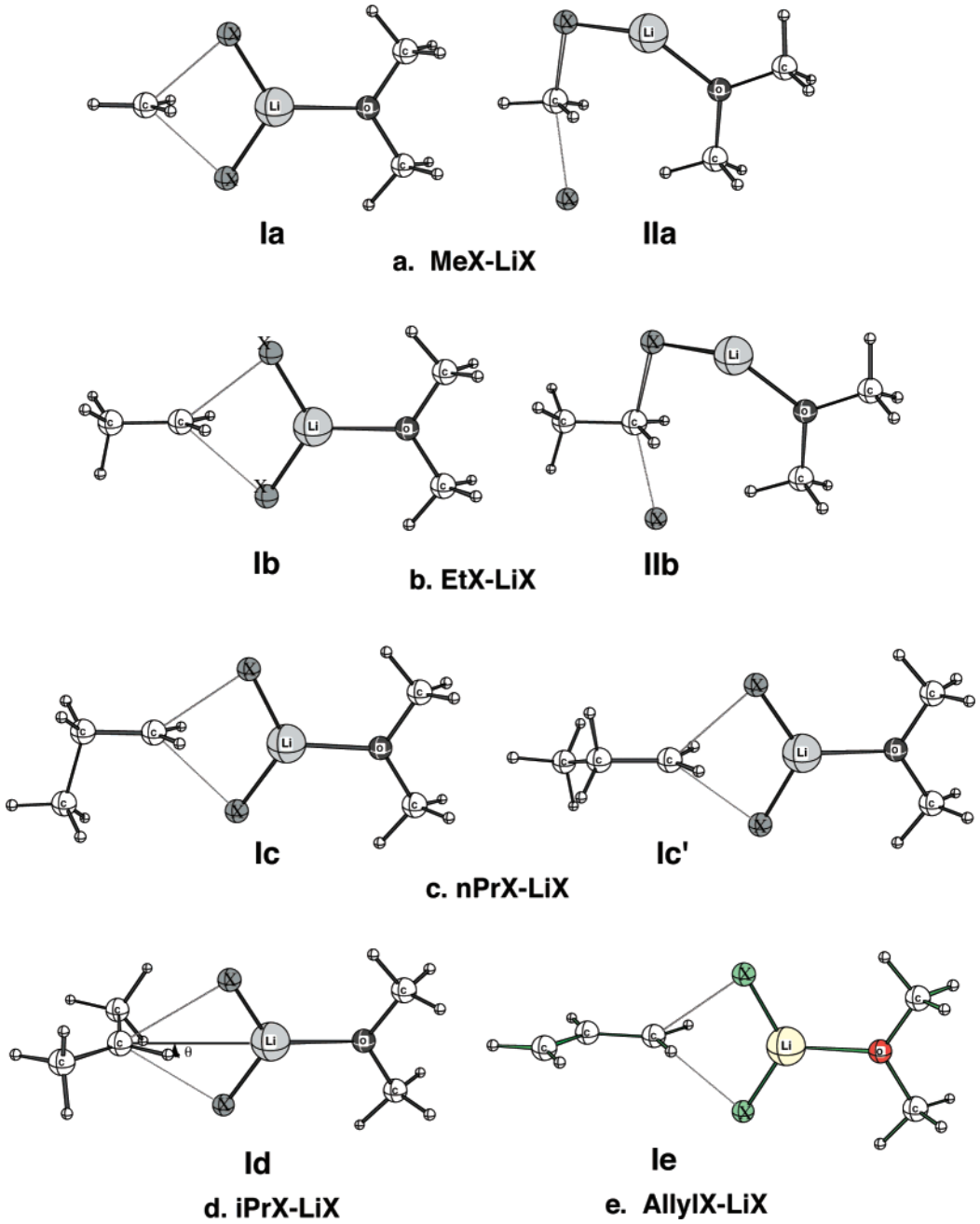

FIGURE 2. Types (I and II) of computed transition structures with monosolvation in RX−LiX·E reaction systems (X = F, Cl, Br).

charge−dipole complex for reactions with anions,[27−29]—or a dipole−dipole complex for reactions with ion pairs.[8] The role of such complexes is less important in solution, at least for highly solvated anions.[30,31] As expected and summarized in Table 1, ether coordination progressively decreases the exothermicity of complex formation, ΔE^{rc}. For example, the energy relative to the reactants of the complex formed from methyl chloride and LiCl coordinated with 0−3 dimethyl ethers is −14.7, −7.7, −4.6, and −3.65 kcal/mol, respectively. This result is readily rationalized by simple electrostatics on the basis that each successive such coordination reduces the net dipole moment of the LiCl; for example, as the Li−X distance gets larger, the Li−O solvent distance decreases. Each additional solvent causes a lengthening of the Li−O bond in exact accord with simple electrostatics. Typical structures are shown in Figure 1, and some bond lengths and angles of the computed reaction complexes are summarized for the MeCl systems at various theory levels in Table 2.

Whenever a computation involves two entities combining, we must be concerned with the effect of the basis set superposition error (BSSE), an effect that arises because each entity in the combined structure has the functions of the other entity to aid in its description; thus, the combined entity is closer to the Hartree−Fock (HF) limit and the computed energy of combination will be artifactually more negative. Galano and Alvarez-

(29) Duke, A. J.; Bader, R. F. W. *Chem. Phys. Lett.* **1971**, *10*, 631−635.
(30) Re, M.; Laria, D. *J. Chem. Phys.* **1996**, *105*, 4584−4596.
(31) Chandrasekhar, J.; Jorgensen, W. L. *J. Am. Chem. Soc.* **1985**, *107*, 2974−2975.

TABLE 3. Some Bond Lengths (Å) and Angles (deg) of Computed Reaction Complexes for Higher Alkyls, RC, at HF/6-31+g*

RC·*n*E	C−X_1	C−X_2	Li−X_1	Li−X_2	Li−O	X−C−X
C_2H_5F−LiF·E	1.420	3.102	1.910	1.634	1.927	70.2
·2E	1.411	3.036	2.012	1.668	1.990; 2.027	72.1
·3E	1.409	3.055	2.028	1.675	1.999; 2.017[b]	71.6
C_2H_5Cl−LiCl·E	1.835	3.697	2.513	2.145	1.905	82.2
·2E	1.824	3.683	2.784	2.199	1.959; 1.982	84.5
·3E	1.817	3.879	5.101	2.245	2.023[a]; 2.011	111.8
C_2H_5Br−LiBr·E	1.999	3.778	2.628	2.300	1.902	85.0
.·2E	1.991	3.756	2.805	2.355	1.951; 1.966	86.6
·3E	1.980	3.804	4.408	2.404	2.012; 2.026; 1.992	93.5
n-C_3H_7F−LiFa·E	1.419	3.095	1.910	1.634	1.928	70.6
g·E	1.422	3.110	1.910	1.634	1.928	70.2
n-C_3H_7Cl−LiCla·E	1.834	3.694	2.512	2.147	1.905	82.7
g·E	1.839	3.713	2.509	2.146	1.906	82.0
n-C_3H_7Br−LiBra·E	1.995	3.764	2.630	2.303	1.902	86.0
g·E	2.004	3.770	2.625	2.301	1.902	85.2
i-C_3H_7F−LiF·E	1.433	3.138	1.902	1.634	1.930	69.4
·2E	1.422	3.104	2.004	1.676	2.009	71.8
·3E	1.406	3.226	4.519	1.681	2.040	106.5
i-C_3H_7Cl−LiCl·E	1.861	3.727	2.497	2.148	1.907	81.4
·2E	1.847	3.708	2.756	2.203	1.962; 1.985	83.7
·3E	1.835	3.875	5.133	2.245	2.021[a]; 2.011	113.0
i-C_3H_7Br−LiBr·E	2.030	3.735	2.621	2.306	1.901	85.4
·2E	2.017	3.727	2.862	2.367	1.965; 1.971	86.4
·3E	1.998	3.788	3.961	2.413	2.012; 2.048; 1.997	89.9
C_3H_5F−LiF·E	1.419	3.140	1.912	1.635	1.926	68.6
·2E	1.409	3.048	2.013	1.667	1.988; 2.025	70.6
C_3H_5Cl−LiCl·E	1.843	3.691	2.508	2.145	1.904	81.6
·2E	1.830	3.667	2.772	2.198	1.980; 1.959	83.6
C_3H_5Br−LiBr·E	2.012	3.755	2.623	2.302	1.901	84.6
·2E	2.000	3.778	2.797	2.352	1.865; 1.953	85.2

[a] The two Li−O bond lengths are identical. [b] One solvent is far away from Li.

Itaboy have shown recently that such BSSE is greatly reduced in going from the 6-311G(d,p) to the 6-311++G(d,p) basis set, that is, by including diffuse functions.[32] This makes sense because the availability of diffuse functions centered on a given entity reduces its need for functions centered on the neighboring entity for its description. To determine how important BSSE might be in our computations that use a single set of diffuse functions (6-31+G(dp)), we calculated the complexation reactions MeCl + LiCl·*n*E = MeCl−LiCl·*n*E at 6-311++G(d,p) for comparison. The results are similar at both HF levels: 6-31+G(d,p), −11.36, −7.71, −4.61, −3.65; 6-311++G(d,p), −11.50, −8.18, −4.84, −4.00 kcal/mol, for $n = 0-3$, respectively. If BSSE was of dominating importance, we would expect ΔE to be more negative for the set with fewer diffuse functions. The two results are actually quite similar with the larger set giving slightly more negative combination energies. We conclude that BSSE is not an important limitation in our use of the 6-31+G(d,p) basis set.

Transition Structures. From the reaction complex, the system then proceeds to reaction via the transition structure. Transition structures for the unsolvated lithium halides have been published previously.[7,8]

At the HF level, two transition structures (TSs) were characterized computationally on monosolvation, i.e., by coordination of one dimethyl ether molecule to lithium (LiX·E). One is the normal C_{2v} TS (type I, Ia, Figure 2) with equivalent entering and leaving groups. The second is a totally unexpected C_s structure (type II, IIa) in which the entering and leaving groups are not equivalent. This nonequivalency apparently violates the principle of microscopic reversibility. In conventional TS theory, such a TS requires a symmetrical intermediate joining the two IIa structures in which the X groups exchange roles. In practice, no such intermediate was found. This type of result will be discussed further below and has been noted previously.[7,33]

The path of the lower-energy barrier in MeF−LiF·E is through the C_s (type II) transition structure ($\Delta E^{ts} = E$(type I) − E(type II) = 5.24 kcal/mol, Table 1). However, in the case of MeCl−LiCl, the two transition structures are of nearly the same energy ($\Delta E^{ts} = -0.06$ kcal/mol) and the normal C_{2v} (type I) transition structure becomes more favored for MeBr−LiBr ($\Delta E^{ts} = -1.10$ kcal/mol). Some of the important TS parameters for MeCl are summarized in Table 2 (a more complete summary is given in Table S1, Supporting Information). A comparison of X−C−X bond angles in all three C_{2v} transition structures shows an order of Br > Cl > F (103.3°, 98.5°, 83.3°) suggesting the importance of an approach to linearity in X−C−X; that is, in the type II TSs, we lose some of the electrostatic interaction between Li^+ and one halide ion but gain a more favorable X−C−X angle. Moreover, the Li−O bond length is shorter in the C_s TSs implying more effective solvation. For example, in the CH_3Cl−LiCl·E reaction system, the Li−O bond length is

(32) Galano, A.; Alvarez-Itaboy, J. R. *J. Comput. Chem.* **2006**, *27*, 1203−1210.

(33) Gonzales, J. M.; Pak, C.; Cox, R. S.; Allen, W. D.; H. F. S., III; Csaszar, A. G.; Tarczay, G. *Chem.−Eur. J* **2003**, *9*, 2173−2192.

TABLE 4. Some Bond Lengths and Angles of HF Computed Type I and Type II Transition Structures for Higher Alkyls[a]

TS, type·*n*E	C−X_1	C−X_2	Li−X_1	Li−X_2	Li−O	X−C−X
C_2H_5F−LiF, I·E	2.338	2.345	1.757	1.755	1.938	79.2
I·2E	2.278	2.281	1.830	1.831	2.013; 2.008	85.9
C_2H_5F−LiF, II·E	1.740	2.119	1.702	3.885	1.874	150.0
II·2E	1.775	2.096	1.737	4.143	1.915; 1.949	156.8
II·3E	1.779	2.076	1.782	4.270	2.002[b]; 2.028	159.2
C_2H_5Cl−LiCl, I·E	2.791	2.782	2.324	2.328	1.905	91.2
I·2E	2.686	2.708	2.511	2.493	1.977	101.9
C_2H_5Cl−LiCl, II·E	2.338	2.707	2.214	4.249	1.846	141.5
II·2E	2.378	2.640	2.288	4.248	1.920	147.0
II·3E	2.369	2.631	2.373	4.831	1.994; 1.997; 2.000	151.0
C_2H_5Br−LiBr, I·E	2.877	2.859	2.480	2.486	1.901	96.6
I·2E	2.804	2.829	2.637	2.625	1.955	104.5
II·2E	2.542	2.745	2.445	4.164	1.901; 1.919	145.3
II·3E	2.511	2.751	2.522	4.836	1.966; 1.987; 1.992	150.0
n-C_3H_7F−LiF, I·E	2.356	2.370	1.754	1.751	1.940	78.5
n-C_3H_7F−LiF, II·E	2.351	2.352	1.755	1.754	1.939	79.0
n-C_3H_7Cl−LiCl, I·E	2.835	2.805	2.312	2.321	1.909	89.6
n-C_3H_7Cl−LiCl, II·E	2.805	2.791	2.323	2.326	1.907	90.9
n-C_3H_7Br−LiBr, I·E	2.869	2.869	2.487	2.487	1.901	96.6
i-C_3H_7F−LiF, I·E	2.646	2.644	1.729	1.729	1.950	67.6
I·2E	1.614		1.773		2.046; 2.057	69.9
I·3E	2.650	2.670	1.766	1.770	2.048; 2.066[c]	68.8
i-C_3H_7F−LiF, II·E	1.849	2.187	1.682	3.987	1.889	150.8
II·2E	1.837	2.166	1.720	4.235	1.938; 1.961	154.3
II·3E	1.870	2.153	1.765	4.394	2.005[b]; 2.053	154.0
i-C_3H_7Cl−LiCl, I·E	3.152	3.155	2.288	2.288	1.919	77.5
I·2E	3.096		2.405		2.008	81.6
II·2E	2.636	2.804	2.257	4.400	1.918; 1.930	133.7
II·3E	2.526	2.824	2.342	5.294	2.016[b]; 1.986	145.5
i-C_3H_7Br−LiBr, I·E	3.171	3.135	2.447	2.451	1.907	83.4
I·2E	3.063	3.076	2.568	2.567	1.986; 1.978	89.4
II·2E	2.731	2.886	2.420	4.386	1.921; 1.907	136.3
II·3E	2.642	2.933	2.513	5.372	1.965; 2.002; 2.007	145.8
n-$C_5H_{11}Cl$−LiCl, I·E	2.808	2.894	2.318	2.300	1.912	88.3
C_3H_5F−LiF, I·E	2.432		1.738		1.948	75.7
I·2E	2.385		1.793		2.045; 2.025	80.0
C_3H_5F−LiF, II·E	1.725	2.105	1.705	3.873	1.872	155.6
II·2E	1.736	2.082	1.738	4.096	1.931; 1.940	157.8
11·3E	1.757	2.050	1.777	4.199	1.998; 2.019; 2.036	159.0
C_3H_5Cl−LiCl, I·E	2.915		2.296		1.917	85.8
I·2E	2.842		2.426		2.002	92.1
11·3E	2.399	2.748	2.380	4.726	1.985; 2.002[b]	141.5
C_3H_5Br−LiBr, I·E	2.989		2.454		1.910	90.6
I·2E	2.943		2.572		1.973	95.5
II·3E	2.518	2.866	2.532	4.762	1.962; 1.983; 1.998	142.7

[a]All other parameters are given in the Supporting Information. [b] The two Li−O bond lengths are identical. [c] One solvent is far away from Li.

1.894 Å for Ia and 1.841 Å for IIa. Thus, solvent coordination is more pronounced in the type II TS. The methyl hydrogens are pulled away from the plane thus indicating their proximity to the corresponding complexes on the potential energy surface (PES). The dihedral angles involving the methyl group reduce to 149.8° for fluoride, to 152.6° for chloride, and to 152.4° for bromide from the ∼180° in the C_{2v} TS. With both transition structures, reaction occurs with inversion of configuration.

At the MP2/6-31+g* level, the type I transition structures for MeF−LiF·E and MeCl−LiCl·E are not first-order saddle points and optimize to the type II TS. At B3LYP, both are TSs for MeCl−LiCl·E with type II more stable by 1 kcal/mol, but another density functional method optimized for S_N2 reactions, mPW1PW91/6-31G*,[22] gives only the type II transition structure. With such variations depending on theory level, we are less concerned about the exact situation with one coordinated solvent than we are with trends. Structures with lithium more fully coordinated with two and three solvents are clearly more important as models and as discussed below tend to favor the type II transition structures.

Higher Alkyls. The higher alkyl halides form reaction complexes with lithium halides entirely analogous to the methyl halides. The general structures are included in Figure 1, and some bond distances and angles are summarized in Table 3.

For the TSs of the higher alkyl reactions, relative energies are included in Table 1 and some structural parameters are summarized in Table 4. In the narcissistic reactions of the ethyl halides, the C_{2v} symmetry can no longer be maintained in the TS and the distances between the central carbon and incoming and leaving groups are slightly different: 2.791 and 2.782 Å for chloride. They are sufficiently close, however, that this structure is clearly of type I and shown as Ib (Figure 1). The second TS, the C_s TS analogue, correspondingly is type II (IIb). This structure becomes relatively higher in energy along the

TABLE 5. Free Energies of Solvation of the Transition Structures as Computed with PCM (Cosmo)[a]

TS	$\Delta G°$sol	$G°$(el)	$G°$(nonel)
MeCl−LiCl, I·2E			
MeCl−LiCl, II·2E	−8.52	−21.42	12.90
MeCl−LiCl, II·3E	−6.94	−22.96	16.02
MeBr−LiBr, II·2E	−7.50	−19.44	11.94
MeBr−LiBr, II·3E	−4.86	−19.94	15.08
EtCl−LiCl, I·2E	0.07	−15.43	15.50
EtCl−LiCl, II·2E	−4.46	−18.86	14.40
EtCl−LiCl, II·3E	−2.85	−19.90	17.05
EtBr−LiBr, I·2E	2.04	−13.16	15.20
EtBr−LiBr, II·2E	−1.61	−15.36	13.75
EtBr−LiBr, II·3E	−0.21	−16.59	16.38
*i*PrCl−LiCl, I·2E	−0.19	−18.15	17.96
*i*PrCl−LiCl, II·2E	−5.04	−20.75	15.71
*i*PrCl−LiCl, II·3E	−2.25	−21.56	19.31
*i*PrBr−LiBr, I·2E	1.55	−15.40	16.95
*i*PrBr−LiBr, II·2E	−2.47	−17.19	14.72
*i*PrBr−LiBr, II·3E	−0.24	−19.20	18.96
allylCl−LiCl, I·2E	−6.09	−21.56	15.47
allylCl−LiCl, II·3E	−5.74	−23.14	17.40
allylBr−LiBr, I·2E	−3.48	−18.77	15.29
allylBr−LiBr, II·3E	−2.99	−19.81	16.82

starting compds	$\Delta G°$sol	$G°$(el)	$G°$(nonel)
LiCl	−43.62	−46.25	2.63
LiCl·E	−10.72	−18.19	7.47
LiCl·2E	−2.62	−14.44	11.82
LiCl·3E	−0.03	−14.18	14.15

[a] Columns give the net, electrostatic, and nonelectrostatic energies as kcal/mol.

series F, Cl, Br, and at Br it disappears; that is, when this structure is used as a starting structure, it optimizes to type I. For monocoordination, the type II structure for EtCl−LiCl·E converges to the type I TS at B3LYP whereas both I and II are TSs at mPW1PW91. For the higher chlorides, both density functional methods give both type I and II TSs, whereas for the bromides, there is a tendency to get only type I.

The anti and gauche conformations of the *n*-propyl group lead to corresponding type I transition structures at HF, one with C_s symmetry and the second C_1 (Ic and Ic′, Figure 1). There is a slight increase in the X−C−X angle in Ic′, whereas C_β−Cγ distances are longer for C_s to minimize steric crowding. The anti conformation is less favorable than the gauch for the starting *n*-propyl fluoride and chloride by 0.06 and 0.40 kcal/mol, respectively, at 6-31+G*, but this difference is enhanced in the S_N2 transition structures with incoming lithium halide to 1.32 and 1.52 kcal/mol, respectively. In other words, the C_s TS (Ic) is less favorable than the C_1 TS, similarly to the reactants (Table 1). However, the order is reversed for bromide where the anti is more favorable by 0.96 kcal/mol. The C_s structure involving the larger bromine is a second-order saddle point with the additional negative frequency corresponding to rotation around the C_β−Cγ bond.

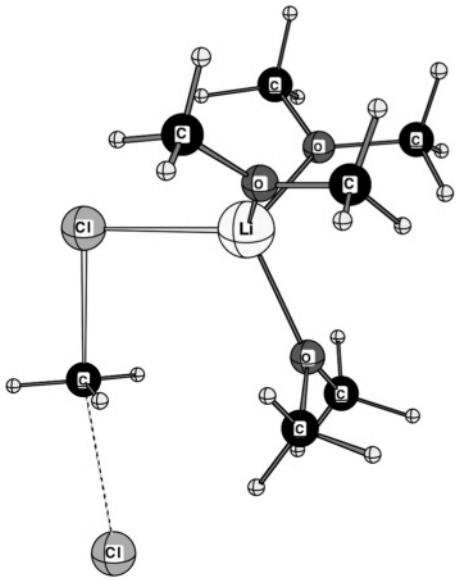

FIGURE 3. Structure of type II trisolvated TS for MeCl + LiCl·3Cl.

C_{2v} symmetry could not be maintained for the type I TS of the isopropyl systems as well. C_{2v} structures are computed to be second-order saddle points with the additional frequency corresponding to the displacement of the hydrogen on the reactive carbon away from the symmetry axis. The displacement angle, θ (Id, Figure 1) is 27.4° for fluoride, 17.4° for chloride, and 25.6° for bromide. At B3LYP, however, both TSs were found for *i*PrCl−LiCl·E with the type II TS almost 10 kcal/mol higher in energy than the type I. Allyl systems will be discussed below.

In general, when compared at the HF level with the gas-phase unsolvated TSs, the key bond lengths of type I TSs around the reaction site are found to be shortened upon monosolvation[7] which makes the solvated TSs somewhat tighter. Among the monosolvated TSs, general trends observed in going toward higher alkyls are: the C−X bond lengths and X−Li−X angles are increased; Li−X1 bond lengths and X−C−X bond angles are reduced. However, the magnitudes of these variations get smaller with higher alkyls (Table 1). For example, Me_2O is coordinated to lithium more strongly in methyl systems where

TABLE 6. Energy Barriers $\Delta E^‡$ (with Respect to the Reaction Complex, MeCl−LiCl·*n*E) and ΔE^* (with Respect to the Separated Reactants, MeCl + LiCl·*n*E) Calculated Using Various Methods

			ΔE^* (kcal/mol)		
method:	RHF	RHF	B3LYP	mPW1PW91	MP2
basis set:	6-31+G*	6-311+G**	6-31+G*	6-31G*	6-31+G*
MeCl + LiCl·EI	40.56	40.33	31.89		
MeCl + LiCl·EII	40.62	40.57	30.82	37.20	36.33
MeCl + LiCl·2EII	36.50	36.40	27.83	33.73	
MeCl + LiCl·3EII	32.27	32.27	25.58	31.20	
			$\Delta E^‡$ (kcal/mol)		
MeCl + LiCl·EI	48.27	48.51	40.62		
MeCl + LiCl·EII	48.34	48.74	39.54	47.28	21.17
MeCl + LiCl·2EII	41.11	41.24	33.06	40.728	
MeCl + LiCl·3EII	35.91	36.26	29.02	35.458	

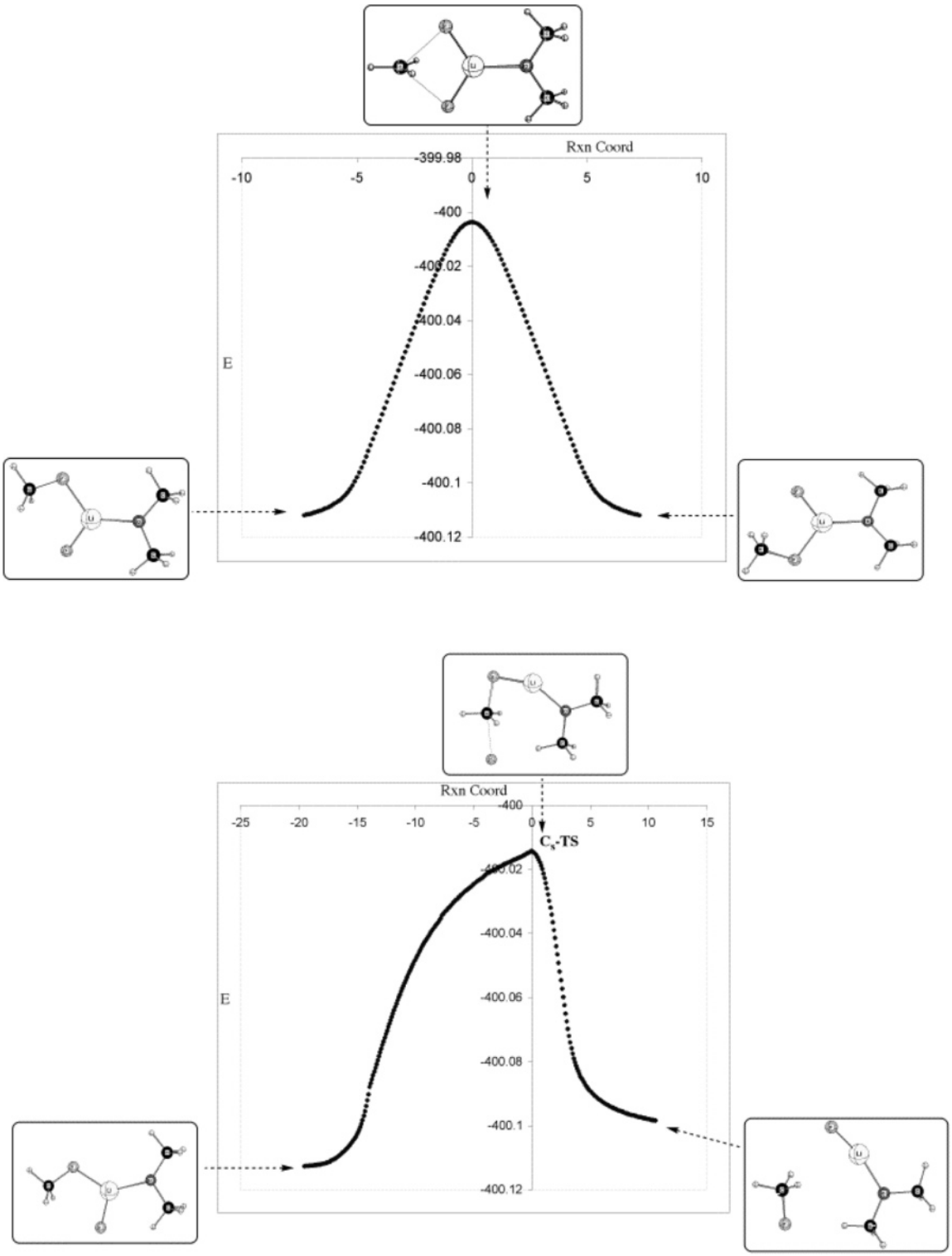

FIGURE 4. IRC results for C_{2v} (type I) and C_s (type II) TSs for MeCl + LiCl·E.

the Li−O distances are shorter, and the bond gets weaker with higher alkyls. The type II transition structures were unexpected. They are more open and might arise because of a better resulting X−C−X angle; in monosolvation, they are less important for higher halides and higher alkyls.

Coordination of Additional Solvents. Structures with more fully coordinated lithium are physically more realistic, and coordination of a second solvent to lithium effects dramatic changes. As summarized in Table 1, the type II TSs with two solvents are relatively much lower in energy than with one solvent at HF and both density functional methods. At MP2 and mPW1PW91, MeF + LiF·2E gives only the type II TS. With the higher RX systems where type II TSs with one solvent could not be found, they could be characterized with two solvents on the PES and they are generally much more stable relative to the monosolvated type I TSs. Moreover, the PCM

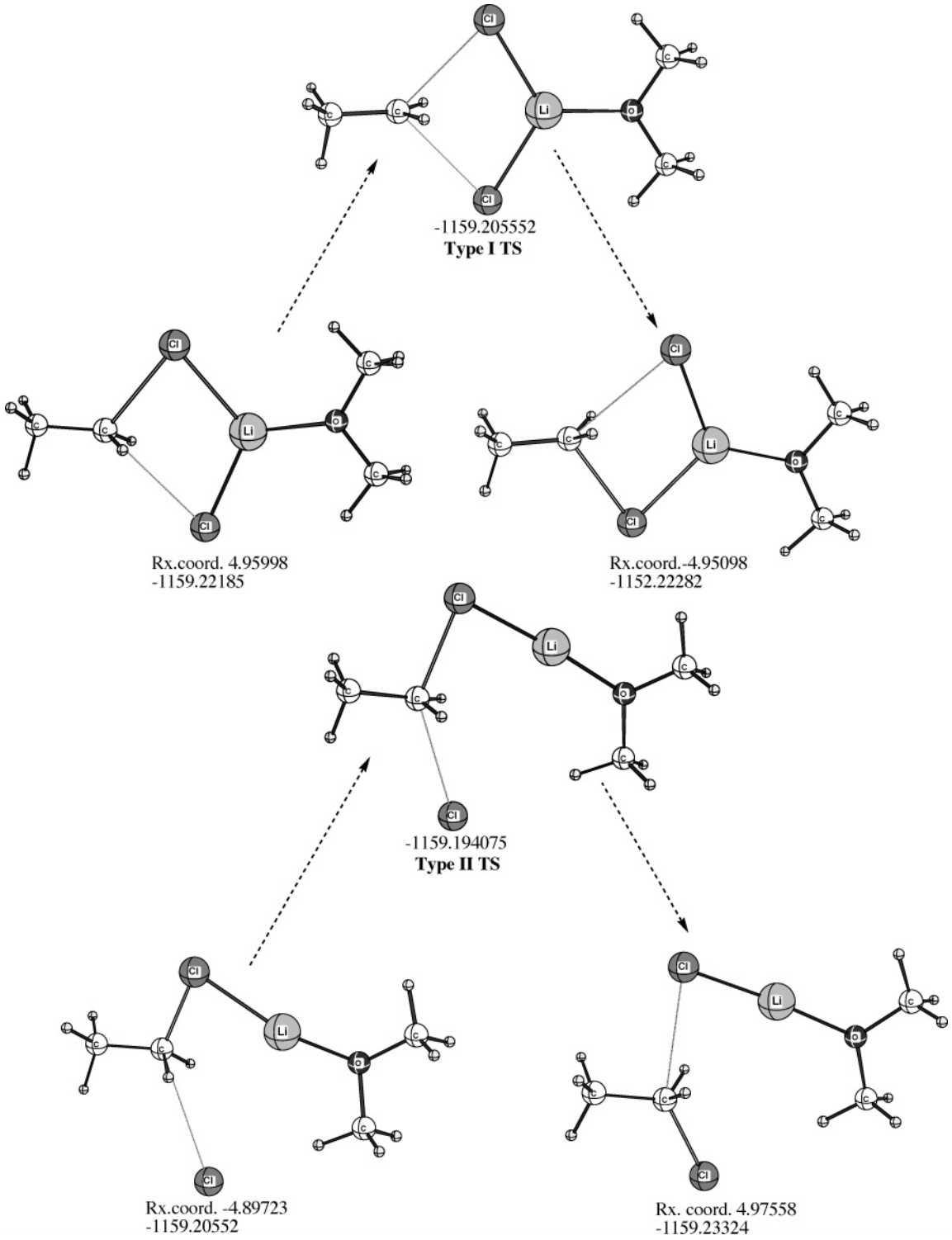

FIGURE 5. Transition states of the EtCl−LiCl·E reaction system and the IRC derived structures in both directions. The reaction coordinates are given in arbitrary units together with the associated energies in atomic units.

dielectric solvation is about 4 kcal/mol more negative for the type II TSs (Table 5). With inclusion of such solvation, all of the type II TSs are more stable than the traditional type I TSs.

For the MeCl−LiCl·*n*E reaction system, several theory levels are compared in Table 6. Additional diffuse functions have only a small effect at the HF level. The reaction barrier with one ether is reduced significantly at MP2, an effect mimicked by mPW1PW91. B3LYP, however, gives reaction barriers much lower than the other methods. Nevertheless, additional solvent coordination results in lower reaction barriers at all the levels studied.

At B3LYP, the type II structures are even more stable relative to type I. For MeCl−LiCl·2E and EtCl−LiCl·2E, the type I structures converged to type II. For *i*PrCl−LiCl·2E, both

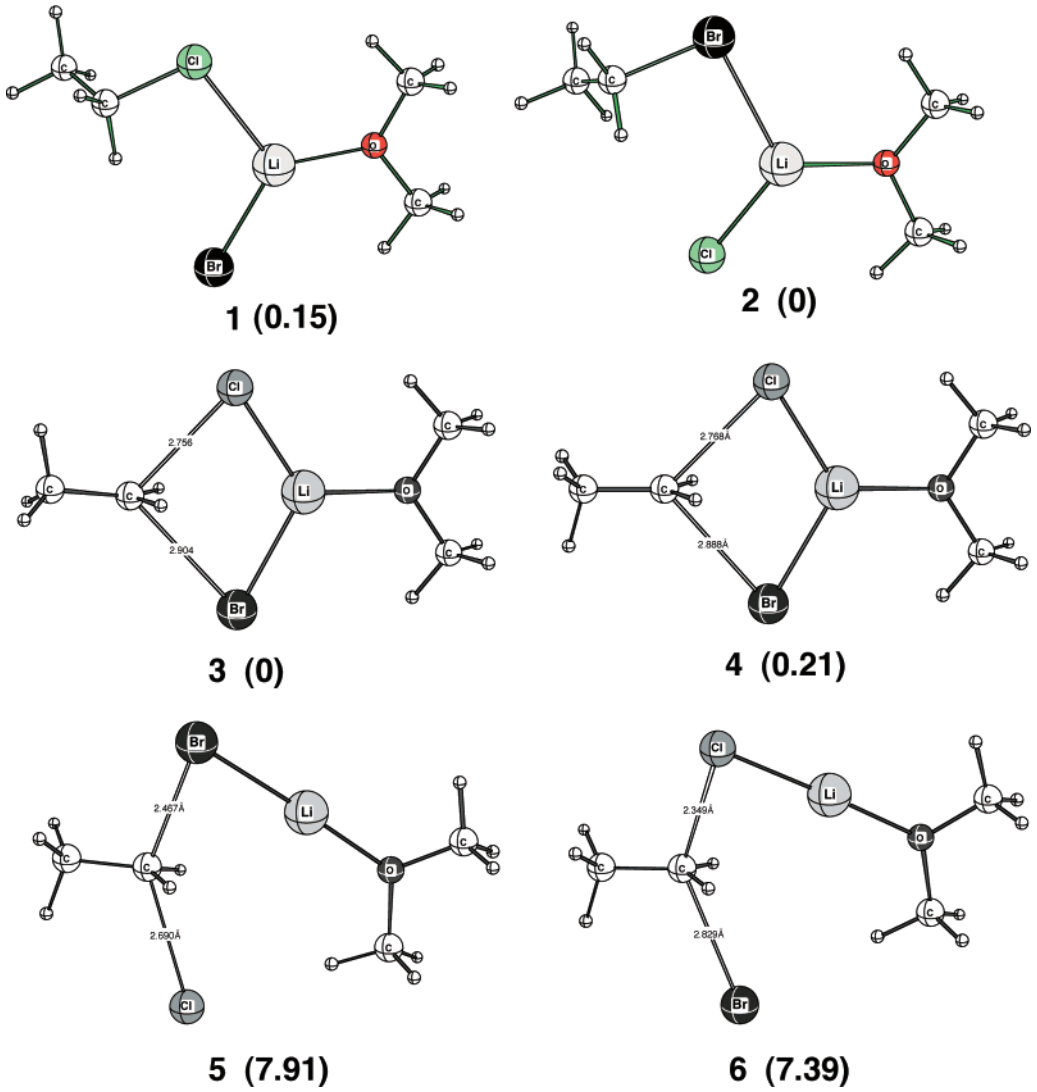

FIGURE 6. Reaction complexes (**1** and **2**) and transition structures (type I, **3** and **4**, and type II, **5** and **6**) obtained in the nonidentity reaction of Me_2O-coordinated LiCl and LiBr with ethyl halide (X = Cl, Br). The relative TS energies (kcal/mol) are given in parentheses.

structures are TSs with type II about 2.5 kcal/mol less stable than type I; at HF, the energy difference is more than 6 kcal/mol.

With three solvents, a type I TS would have a formally pentacoordinated lithium. Optimization of such a structure resulted generally in progressive loss of one ether to give the disolvated type I TS, $MeCl_2$−Li·2E. With the fluoride systems, MeF−LiF·3E and *i*PrF-LiF·3E, starting with a type I TS gave a stationary point on the PES consisting of a type I RF_2−Li·2E TS with a molecule of Me_2O far away, apparently as a dipole complex. These structures were not considered further but are recorded in Table S6 (Supporting Information). All of the reaction systems did give type II TSs with three solvent molecules. The TS for MeCl−LiCl·3E is shown as an example in Figure 3. Shown clearly is the tetragonal coordination about lithium and the shorter C−Cl bond distance to the coordinated chloride compared to the free chloride. The dielectric solvation energies of these type II TSs are a little lower than with two solvents, but so are the corresponding energies of LiX·3E compared to LiX·2E (Table 5).

The significant energy changes computed upon di- and trisolvation are given in Table 1. The energy barriers with respect to the reactants show an increase in going from the gas phase to monosolvation except for the type II MeF−LiF TS. The fluoride reactions are frequently atypical, and we will emphasize the chemistry of the synthetically more important chlorides and bromides. For these systems, coordination of solvent increases the reaction barriers relative to the unsolvated gas phase but the barriers, particularly for di- and trisolvation, are all in a chemical range of <30 kcal/mol. All of the barriers show the trend Me > Et > *i*Pr, which is an apparent difference from experiment, although with LiX·3E the differences are small. The dielectric solvation energies of the methyl TSs are all significantly more negative than for the higher systems and have the effect of reducing the relative reaction barriers for methyl; that is, with inclusion of such solvation, we approach or reach the experimental reactivities of Me > Et. At B3LYP also, the reaction barrier for EtCl is about 1 kcal/mol lower than for MeCl, but inclusion of dielectric solvation again makes the methyl barrier lower.

Reaction Mechanism. The S_N2 reaction can be regarded simply as the combination of the two reactants to form a complex that then isomerizes to produce the transition state. Continued reaction then gives the reaction complex in which

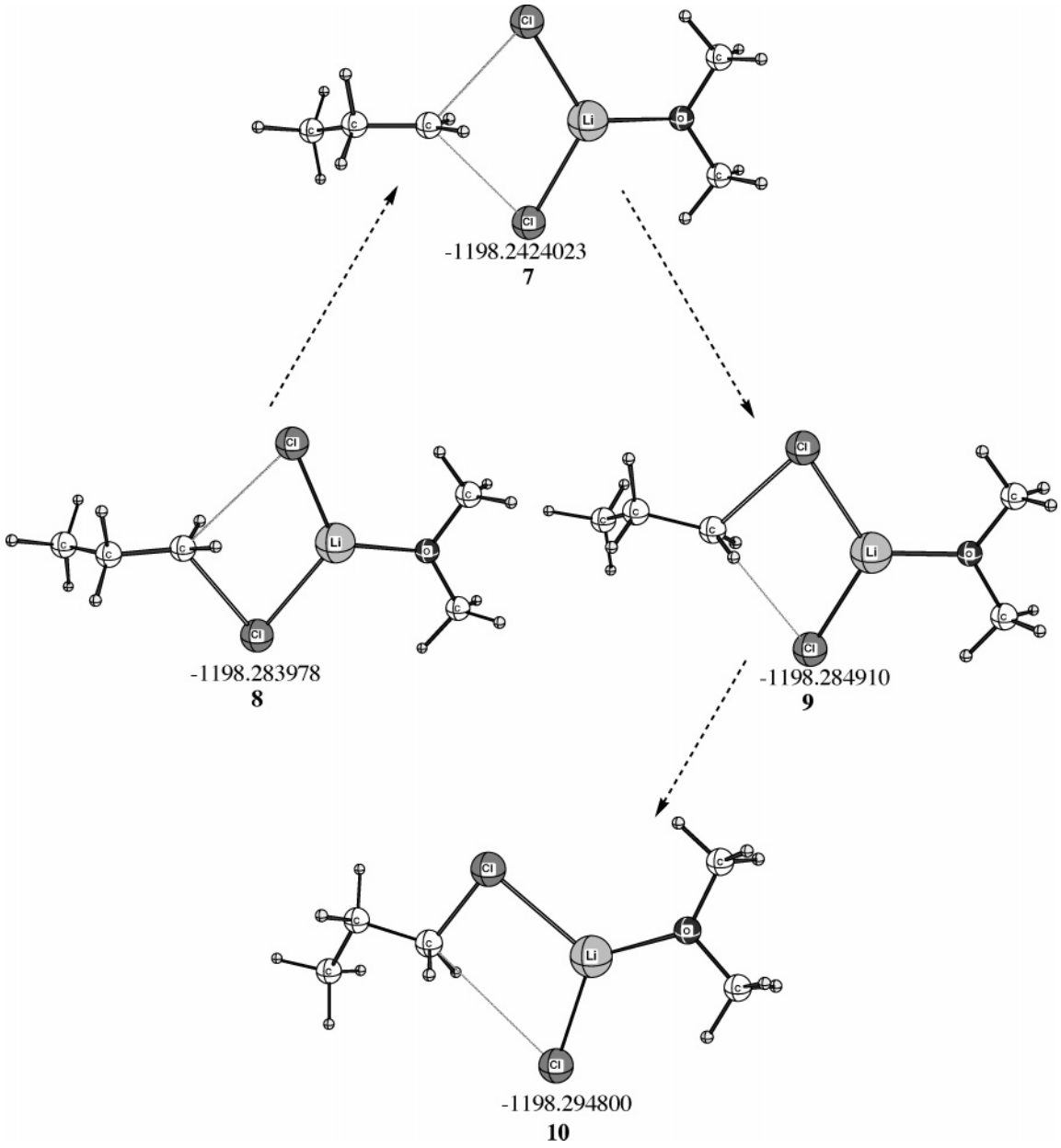

FIGURE 7. IRC derived structures for *n*-propyl chloride with LiCl·E.

the two halides have exchanged places. Because the reaction complex is generally lower in energy than the separated reactants, the transition barrier is higher for the complex. Nevertheless, with three-coordinated solvents, the difference is relatively small. For example, with three ethers, the complexation energy, ΔE^{rc}, for RCl−LiCl·3E is less than 4 kcal/mol. The corresponding value for $\Delta G°$ is expected to be substantially lower because of the loss of translational entropy in forming the complex. Consequently, energy trends are much the same relative either to separated reactants, ΔE^{*}, or to the reaction complexes, $\Delta E^{‡}$. The various computed energy barriers are given in Table 1. The unsolvated gas-phase results are also given in Table 1 for comparison and were calculated from the total energies given previously.[7] Overall, the trends of the various energy barriers across different alkyl halides are similar.

It is convenient, however, to regard the transition structure as arising by a rearrangement of the reaction complex. This approach is straightforward for the traditional type I transition structures, but we must also consider how the process works for the unusual type II structures. To characterize these different reaction paths, we computed the intrinsic reaction coordinate (IRC).[8] This method follows along the reaction coordinate in both directions from the TS. Because the method is an expansion process, even with small reaction increments the cumulative errors do not permit going all the way to reactants and products. However, important insights do result. Because determining the IRC is computer intensive, we applied the method only to monosolvation, but the results are expected to be general. For the reaction, MeCl + LiCl·E, via the C_{2v} type I TS, the IRC is normal. The reaction path is symmetrical in both directions (Figure 4). The final structures at both ends are minima on the PES and approach that of the encounter complex between LiCl·E and MeCl, after methyl rotation. The IRC of the type II C_s TS is totally different and is asymmetric. In one direction, it

TABLE 7. CC Bond Lengths in TS Structures of Allyl Chloride with Various Nucleophiles

nucleophile	r(C−C), Å	R(C═C), Å
Cl^{-}[a]	1.463	1.322
LiCl[a]	1.407	1.347
LiCl·E	1.412	1.344
LiCl·2E	1.418	1.341
LiCl·3E	1.447	1.327

[a] Ref 30.

reaches a reaction complex structure similar to that obtained for the C_{2v} TS, but the other end goes to a more separated structure. This structure is not a stationary point on the PES but is probably en route to the same reaction complex albeit by a longer path. The apparent violation of microscopic reversibility is resolved by allowing the reaction to start at either end. Note that at no point along the reaction path do the two halides become equivalent.

The EtCl−LiCl·E type I TS shown in Figure 5 has one chloride (leaving group) staggered with respect to the methyl group and another (entering group) eclipsed. IRC calculations on this TS show that continued reaction along this path would lead to an eclipsed conformation of EtCl that is itself a TS. As discussed previously,[7] at some point along the reaction pathway, an independent rotation of the methyl group must occur to yield a normal staggered product. The same situation occurs with the type II TS shown in Figure 5. In one direction from the TS, the lithium is coordinated to the leaving (staggered) chloride (shorter r(C−Cl)). In the other direction, the shorter C−Cl bond is eclipsed to the methyl group, and an independent rotation is again required. Alternatively, this process could happen in reverse to accommodate the principle of microscopic reversibility; that is, in the reverse process, rotation takes place before the S_N2 TS in both cases. To understand this process more clearly, we analyzed a nonidentity reaction, EtCl + LiBr·E = EtBr + LiCl·E, which involves two different reaction complexes. The result is summarized in Figure 6. The two reaction complexes, **1** and **2**, have similar structures and almost identical energies. These lead to two type I and two type II TSs differing in whether the Cl or the Br is eclipsed to the methyl group. TS **3** is the most favorable structure with the lowest energy, but **3** and **4** differ in energy by only 0.21 kcal/mol.

The type II transition structures **5** and **6** show that as the lithium bromide attacks the reactive carbon center of EtCl a favorable interaction exists between the methyl hydrogen and the attacking halide initially; however, further advance of the attacking halide toward the methyl carbon results in unfavorable interaction between the in-plane methyl hydrogen, and the attacking halide forces the rotation of the methyl group. This is substantiated by calculating the structures with the halide of lithium halide and both the carbon atoms coplanar with the hydrogen of the terminal methyl group (X−C−C−H, dihedral angle of zero), which is found to be a second-order saddle point in which the first imaginary frequency corresponds to the S_N2 reaction and the second corresponds to the rotation of the methyl group. Thus, these transition structures lead to staggered products but are preceded by a rotation. The rotation that occurs during the substitution reaction has stereochemical consequences. The IRC results obtained for the TS of *n*-propyl chloride are summarized in Figure 7. The starting point is **7**, the skew C1 TS (type I) that leads to two structures in different directions from the TS. One, **8**, is similar to a corresponding structure in the ethyl case. The other, **9**, is itself a TS (with one imaginary frequency), and the IRC on it leads by C−C bond rotation to **10**, a fully staggered product.

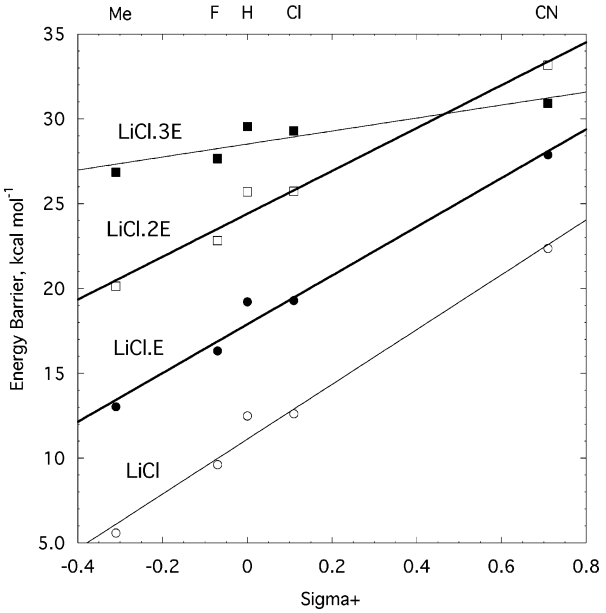

FIGURE 8. Reaction barriers for trans-γ-substituted allyl chlorides with LiCl·nE (n = 0−3). Regression lines shown are LiCl: 11.116 ± 0.414 + (16.159 ± 1.179)σ + (R^2 = 0.984) (ref 34). LiCl·E: 17.89 ± 0.407 + (14.374 ± 0.158)σ+ (R^2 = 0.981). LiCl·2E: 24.404 ± 0.407 + (12643 ± 1.158)σ + (R^2 = 0.975). LiCl·3E: 28.521 ± 0.366 + (3.829 ± 1.041)σ + (R^2 = 0.819).

One important distinction between the type I and type II TSs that emerges from the data in Table 1 is that for type I structures additional solvent coordination *increases* the reaction barrier whereas for type II structures additional solvent coordination *decreases* the reaction barrier.

Allyl. With one or two solvents, only for allyl fluoride with LiF·E and LiF·2E could type II TSs be characterized, but in these structures, the vinyl group is perpendicular to the reaction center and not conjugated with it. These structures might be artifacts and are not considered further. The type I TSs are essentially normal. The C−X and Li−X bond lengths of the allylic type I TSs lie between the *n*-propyl and isopropyl systems. The energy barriers also follow a similar trend, falling slightly higher and closer to *i*-propyl systems.

We had noted previously that the C−C bond lengths in the gas-phase S_N2 reactions of allyl halides with halide ions are similar to those of the starting allyl halides and that no conjugation between the reactive center and the double bond is apparent.[34] This result was rationalized on the basis that the electrostatic effect of the halide ions prevents polarization of cationic charge to the distant γ-carbon. This proscription is reduced by the electrostatic effect of Li^+ in the LiX ion pair TS with resulting shortening of the C−C single bond and lengthening of the C═C double bond in the allyl moiety. Coordinated solvent dipoles oppose this effect of Li^+, and accordingly, the TSs of allyl chloride with LiCl coordinated with one to three dimethyl ethers show a progressive change toward normal single and double bond lengths (Table 7). This progression is also manifest in substituent effects.

(34) Streitwieser, A.; Jayasree, E. G.; Leung, S. S. H.; Choy, G. S. C. *J. Org. Chem.* **2005**, *70*, 8486−8491.

We showed previously that the reactions of trans-γ-substituted allyl chlorides with a chloride ion follow Hammett σ-constants with electron-attracting groups lowering the reaction barrier.[34] Reaction with LiCl, however, follows $\sigma+$ and with the opposite sign of ρ; that is, electron-attracting groups increase the barrier to reaction. Substituent effects with LiCl·*n*E are summarized in Figure 8. The reactions still follow $\sigma+$ (one talisman is that the F-substituent is effectively electron-donating) but with a gradual reduction of ρ with increasing *n*. This result parallels that of the C−C bond lengths mentioned above. With the type II TS of allyl chloride − LiCl·3E, the Li^+ is now farther away and has reduced effectiveness in allowing polarization of cationic charge to the γ-position. The result is a relatively low value of ρ.

Conclusions

Microsolvation studies of ion pair S_N2 reaction of alkyl halides resulted in symmetrical (type I) and unsymmetrical transition states (type II): the former TSs disappear and the latter remain with increased solvation. Consequently, reaction paths of type II TSs are unsymmetrical. The type II TSs also show somewhat greater dielectric solvation, but the differences are relatively small. Successive solvent coordination reduces the energy barriers for type II TSs. One important outcome of this study is the importance of considering coordination solvation of lithium salts in donor solvents; such coordinated structures are probably much better models for experimental chemistry.

Acknowledgment. This work was supported in part by grants from the National Science Foundation.

Supporting Information Available: Tables of computation results and complete ref 21. This material is available free of charge via the Internet at http://pubs.acs.org.

JO0625709